JOURNAL OF AIRCRAFT
Vol. 35, No. 2, March–April 1998

Fully Three-Dimensional Transition Prediction on Swept Wings in Transonic Flows

Marc Langlois*
Bombardier Aerospace Group, Dorval, Quebec H3C 3G9, Canada
Christian Masson†
École de Technologie Supérieure, Montreal, Quebec H3C 1K3, Canada
and
Ion Paraschivoiu‡
École Polytechnique de Montréale, Montreal, Quebec H3C 3A7, Canada

A stability analyzer for transition prediction over arbitrary three-dimensional wings operating in the transonic regime is proposed. This analyzer is used to illustrate the importance of including the effects of spanwise pressure gradient in transition predictions over such configurations. To this end, three calculation methods were employed: 1) a three-dimensional Euler solver, 2) a three-dimensional boundary-layer solver, and 3) a numerical method for the solution of the linear stability equations based on the temporal formulation. The influence of spanwise pressure gradients is illustrated by the application of this stability analyzer to the flow about the NASA AMES and ONERA-M6 wings. The pertinence of using a fully three-dimensional method rather than the simpler conical-flow calculations is demonstrated. The differences between the fully three-dimensional and conical-flow results are of the same order as the curvature or nonparallel effects.

Nomenclature

b = wingspan, m
C_p = pressure coefficient
c = wing mean chord, m
f = frequency, Hz
k = wave-vector module
M_∞ = freestream Mach number
n = amplification factor
Q = mean flow quantity
q = instantaneous flow quantity
Re_c = Reynolds number, $U_e c/\nu_e$
t = time
U_e = inviscid flow velocity, m/s
u, v, w = instantaneous velocity components
$\boldsymbol{V}_{gr}$ = group velocity vector, real part
V_∞ = freestream velocity, m/s
x, y, z = local Cartesian coordinates
α = angle of attack
α, β = wave-vector components
γ_i = spatial growth rate
ν_e = kinematic viscosity, m^2/s
ψ = wave-vector direction with respect to the inviscid streamline
ψ_e = orientation of the inviscid streamline with respect to the chordwise direction
ω = pulsation of the perturbation

Subscripts
i = imaginary part
r = real part

Superscript
$\sim$ = perturbation quantity

Received Feb. 1, 1997; revision received Oct. 17, 1997; accepted for publication Oct. 28, 1997.

*Staff Engineer, Advanced Aerodynamics. Member AIAA.
†Associate Professor, Mechanical Engineering Department. Member AIAA.
‡Chair Professor, J.-A. Bombardier Aeronautical Chair. Associate Fellow AIAA.

Introduction

THE transition from laminar to turbulent flow is an essential aspect of fluid dynamics, in relation to drag reduction. The physical processes associated with transition are not yet fully understood, as pointed out by Saric[1] in his review of experimental research in transition. It is nonetheless an established fact that a significant reduction of the skin friction drag can be obtained by maintaining a laminar flow over the longest extent possible of the wing. This is realized by the use of natural laminar flow (NLF) airfoils and laminar flow control (LFC) technologies such as suction and wall cooling.

The capability to predict transition is thus essential to wing-design engineers. The linear stability theory, along with the empirical e^n method, provides an appropriate framework for transition predictions over wings in the cruise regime. Numerical methods for the solution of the linear stability equations have been developed.[2–5] These methods were mostly applied to infinite swept wings or conical wings. Only a few recent efforts are presented in the literature for the analysis of arbitrary geometries. Spall and Wie[6] studied the stability of the boundary layer over the nose of a general aviation aircraft in the incompressible flow regime. Iyer et al.[7] considered the attachment-line problem on the leading edge of a swept transonic wing.

The authors have developed a stability analyzer (SCOLIC) based on the temporal and spatial formulations of the linear stability theory.[8,9] SCOLIC also originally used the conical-wing assumption and was therefore appropriate for the prediction of transition location on two-dimensional sections and three-dimensional conical swept wings only. It has now been extended for arbitrary three-dimensional flows and integrated into a stability analysis package that includes a three-dimensional Euler solver and a three-dimensional boundary-layer solver.

This paper presents results that have been obtained with this stability analyzer. The importance of undertaking fully three-dimensional calculations is demonstrated by comparing the results obtained with the three-dimensional stability analyzer to conical-flow solutions.

Stability Analysis

The linear stability theory analyzes the characteristics of the instabilities in the mean laminar flow near the surface of interest. Transition prediction is composed of three tasks: 1) the calculation of the external inviscid flowfield using an inviscid-flow solver, 2) the accurate calculation of the viscous flowfield in the vicinity of the body using a boundary-layer solver, and 3) the solution of the linear stability equations.

Flow Calculations

The inviscid flowfield is obtained through the solution of the three-dimensional unsteady Euler equations. The numerical method chosen here to solve the equations is based on a finite volume cell-centered formulation.[10] A structured O–H grid is used to discretize the calculation domain. To compute the viscous flow near the surface, a finite difference boundary-layer code based on the characteristics method[11] is used.

In the complete three-dimensional calculation procedure used in this work, the surface velocity distribution needed to conduct boundary-layer calculations is directly given by the Euler solver. On the other hand, the procedure typically used to compute surface velocities in conical-flow calculations consists of solving the surface Euler equations expressed in the conical-wing coordinate system[12]:

$$\frac{dw_e}{d\theta} = -u_e = -\sqrt{u_s^2 - w_e^2} \tag{1}$$

where u_e is the circumferential (chordwise) surface velocity, w_e is the radial (spanwise) surface velocity, u_s is the resultant inviscid velocity obtained from the surface pressure by using the compressible Bernoulli equation, and θ is the circumferential coordinate.

Transition Prediction

Linear Stability Theory

For a local Cartesian coordinate system, the instantaneous flow variables, i.e., the velocity components u, v, w in the streamwise x, wall-normal y, and crossflow z directions, the pressure p and the temperature T, are assumed to be of the form

$$q(x, y, z, t) = Q(y) + \tilde{q}(y)e^{i(\alpha x + \beta z - \omega t)} \tag{2}$$

where $Q(y)$ is the laminar mean profile, $\tilde{q}(y)$ is the perturbation amplitude, α and β are its wave numbers, and ω its pulsation (complex frequency).

The problem is formulated using the parallel flow assumption. By neglecting the non-linear and higher-order terms, the problem can be expressed as a homogeneous system of five linear, second-order ODEs. Given homogeneous boundary conditions, the task reduces to the solution of an eigenvalue problem: nontrivial solutions exist only for certain combinations of the parameters α, β, and ω. In general α, β, and ω are complex numbers, which corresponds to six real parameters. In the temporal stability theory used here, α and β are assumed to be real. The real part of ω, ω_r, is the frequency of the perturbation, and its imaginary part ω_i yields the perturbation temporal growth rate.

A finite difference method using a staggered mesh is employed in this work to discretize the linear stability equations. For given α and β, the system of equations is amenable to a linear eigenvalue problem in ω.

e^n Method

The linear stability theory allows the calculation of the stability characteristics of a laminar flowfield. However, the main objective of this work is transition prediction. The main assumption regarding transition prediction is that there exists a critical amplification of the disturbances at the transition location. The amplitude ratio A/A_0 can be calculated assuming that the growth of the disturbance from its initial amplitude A_0, to the critical value A_{cr}, can be predicted by the linear stability characteristics. The amplitude ratio, or the more commonly used amplification factor, $n = \ell n(A/A_0)$, is calculated by integrating γ_i along the path of propagation that is parallel to $\boldsymbol{V}_{gr}$

$$n(s) = \int_{s_0}^{s} -\gamma_i \, ds \tag{3}$$

where s is the position on the wing surface and s_0 is the point of inception of the perturbation ($\gamma_i = 0$). The real part of the group velocity is given by

$$\boldsymbol{V}_{gr} = \left(\frac{\partial \omega_r}{\partial \alpha}, \frac{\partial \omega_r}{\partial \beta}\right) \tag{4}$$

When integrating the n factor, the main difference between a quasi-three-dimensional stability analysis and a fully three-dimensional one lies in the selection of the boundary-layer solutions. On an infinite-span wing, the similarity of the solution in the spanwise direction allows the use of a single spanwise section, and the calculations proceed in the streamwise direction one station at a time. The same applies for a conical wing. On an arbitrary three-dimensional wing, there is no such spanwise similarity. It is therefore necessary to use a selection procedure based on the group velocity. Figure 1 illustrates the procedure used in SCOLIC: the n-factor integration points are defined by following the direction given by the group velocity until the intersection with a grid line where new stability calculations are performed using the boundary-layer profiles from the nearest grid point. This strategy was adopted to avoid interpolation of the boundary-layer profiles between neighboring stations. The calculation procedure starts near the leading edge and the inception point, where the n-factor integration begins, is automatically determined by the code.

The n-factor calculation is done under the constraint of constant dimensional frequency f. A finite number of frequencies are selected, and an n factor is calculated for each of them. The frequency that reaches the critical n factor first is considered the most relevant frequency for the prediction of transition location.

In the temporal stability theory used here, there are four independent parameters: α, β, ω_r, and ω_i. The eigenvalue prob-

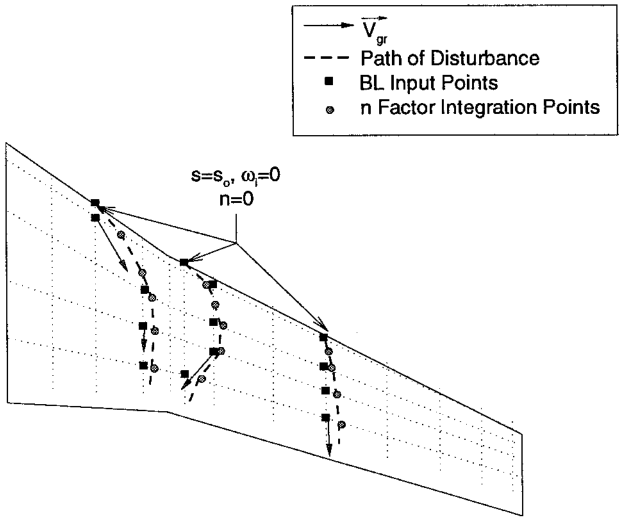

Fig. 1 Fully three-dimensional n-factor integration procedure.

lem provides two real relations. In the calculation of the n factor, the frequency ω_r is given. Therefore, an additional relation (or constraint) is needed to close the problem. This additional constraint is provided by the maximization of the temporal growth rate ω_i (envelope method).

The correlation of the amplification factor with the transition location is the basis of the so-called e^n method. The critical value n_{cr} is not universal and depends on the type and amplitude of the forcing disturbances.[13] For flight conditions (low background turbulence levels), a mean value of 15 has been observed experimentally,[14] when the n factor is calculated using the envelope method.

The numerical procedures implemented in the code SCOLIC have been validated by comparisons of the results with those from other linear stability analysis codes. Such comparisons are reported in Refs. 8 and 9.

Results and Discussion

To demonstrate the capability of the proposed stability analyzer to predict transition over an arbitrary wing, the latter was applied to the transonic flow on two different wings: the NASA AMES swept wing and the ONERA-M6 wing. The whole calculation procedure will be presented for the NASA AMES wing, with results for both the lower and upper surfaces, whereas only n-factor distributions will be given for the ONERA wing. These wings are described in Ref. 15.

NASA AMES Swept Wing

The NASA AMES swept wing is representative of actual geometries encountered on commercial aircraft. It is composed of two sections: the inboard section has a leading-edge sweep of 36 deg and a trailing edge sweep of 3.6 deg, while the sweep angles of the outboard section are 27 and 17 deg for the leading and trailing edges, respectively. The wing profile and twist vary along the span. Calculations were performed at $M_\infty = 0.833$, $\alpha = 1.75$ deg, and $Re_c = 14.3 \times 10^6$ (based on the mean chord, $c = 2.42$ m).

The pressure distribution on the wing surface was obtained using the three-dimensional Euler solver with a grid of $121 \times 31 \times 48$ points. The pressure coefficient distribution on the suction and pressure sides of the wing is presented in Fig. 2. It is worth noticing at this point that the pressure field over this wing is far from being conical because significant spanwise pressure gradients are observed in Fig. 2, particularly on the inboard section, and that a strong shock is located far aft along the whole span of the wing upper surface.

Streamwise and crossflow velocity distributions are presented in Fig. 3 at three x/c locations in the 17.2% span section. To assess the importance of the spanwise pressure gradients, the three-dimensional results are compared with conical-flow solutions, as were previously used.[8] These were obtained by first calculating the surface velocities by integration of the surface Euler equations [Eq. (1)], in which the conical-flow assumption is used. These edge velocities are then used as boundary condition in the solution of the conical boundary-layer equations. Figure 3 shows significant differences between the two solutions, which increase when going downstream. It can be clearly seen on Fig. 4 that the edge velocities calculated with the conical surface Euler equations [Eq. (1)] differ, mainly in orientation, from those predicted by the three-dimensional inviscid solution. The differences between the fully three-dimensional and conical boundary-layer solutions are caused primarily by the calculation of the surface velocities rather than by the assumption of a conical pressure field in the boundary-layer equations. This conclusion was substantiated by conducting fully three-dimensional boundary-layer calculations with the velocities calculated using the conical surface Euler equations: The results were essentially identical to the pure conical solutions of Fig. 3.

The transition prediction procedure used in this work begins with the determination of the complex dispersion relation $\omega(\alpha, \beta)$ at some selected points on the wing to identify the types of instabilities present and their location. The dispersion

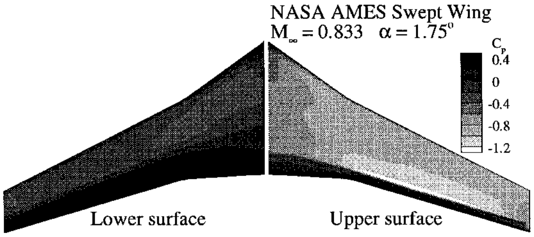

Fig. 2 Surface pressure distribution.

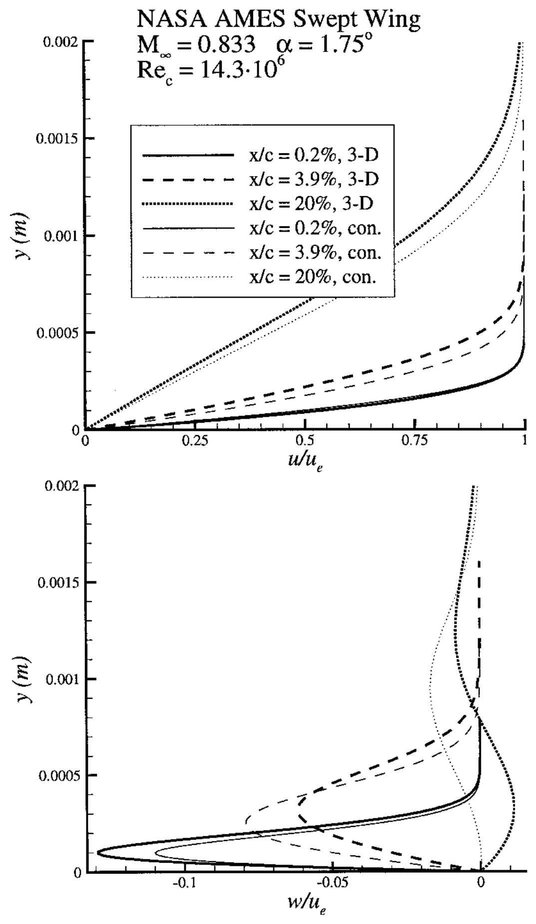

Fig. 3 Boundary-layer profiles at z/b = 17.2%.

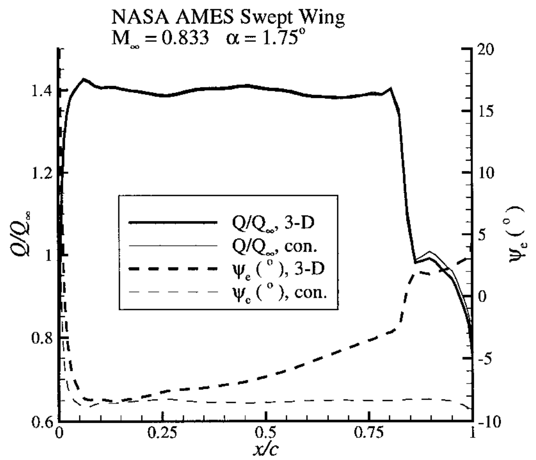

Fig. 4 Surface velocity distribution at z/b = 17.2.

relations in the unstable region at x/c = 2 and 20% (z/b = 17.2%) are illustrated in Fig. 5. The complex dispersion relations of Fig. 5 are expressed in terms of the wave number module $k = \sqrt{\alpha^2 + \beta^2}$, and the wave orientation with respect to the streamline $\psi = \arctan(\beta/\alpha)$. The different shades of gray represent the nondimensional temporal amplification rate ω_i while the nondimensional frequency ω_r is represented by the numbered lines. The graphical representation in Fig. 5 is a valuable tool in helping to choose the critical frequencies and to visualize the physical mechanism. For example, the complex dispersion relation near the leading edge (x/c = 2%), typical of regions with crossflow instability, is shown in Fig. 5a. The unstable wave orientation lies in the range 50 deg $\leq \psi \leq$ 95 deg, and the maximum temporal growth rate ω_i is obtained at (ψ, k) = (80 deg, 0.45). The complex dispersion relation downstream of the leading edge (x/c = 0.20), typical of regions where both crossflow and streamwise instabilities exist, is shown in Fig. 5b. At such locations, multiple local maxima can be noted within the unstable region. In this specific case, one of the local maxima corresponds to a crossflow instability at (ψ, k) = (87 deg, 0.55), and the other two are mainly related to streamwise instabilities at (ψ, k) = (35 deg, 0.15) and (−65 deg, 0.25).

The existence of multiple local maxima makes the n-factor value nonunique because, in principle, crossflow and streamwise instabilities can be treated separately. We adopted the envelope method strategy, however, which considers the crossflow and streamwise instabilities as additive. This strategy was chosen based on past success reported in the literature.

The selection of the critical frequencies to be used in the n-factor calculations is directly related to the evolution of the local maxima downstream of the leading edge. Once a local maximum is located at a (x, z) location, it is possible to follow it downstream using a free maximization procedure of ω_i in the (α, β) space. Typical results of such a tracking are presented in Fig. 6. Based on these results, it has been determined that the most critical frequency for the case studied is 5.0 kHz, and is essentially invariant along the span.

Contours of the computed n factor for that given frequency are shown in Fig. 7. Much of the growth of the n factor from the leading edge is effected by crossflow instabilities, though mixed crossflow/streamwise instabilities have a significant contribution on the outboard section of the wing, with a switch from the former instabilities to the latter at about 10% chord. An interesting feature that can be observed here is the influence of the junction between the two sections of the wing, where a local maximum of the n factor can be seen on the upper surface. This is absent from the results obtained with a locally conical method,[8] as shown in Fig. 8. This also shows levels of amplification that differ much from the three-dimensional solution, the latter being lower on the inboard section and higher on the outboard. These differences are as important as those that typically result from the inclusion of curvature or nonparallel effects.[16,17]

A typical value of the critical n factor for low-disturbance flight conditions is n_{cr} = 15.[14] Figure 9a shows the transition

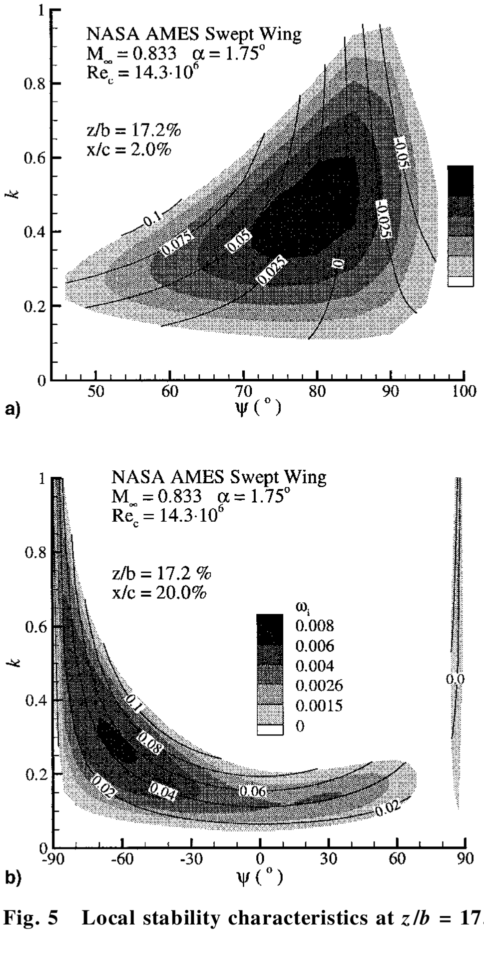

Fig. 5 Local stability characteristics at z/b = 17.2%.

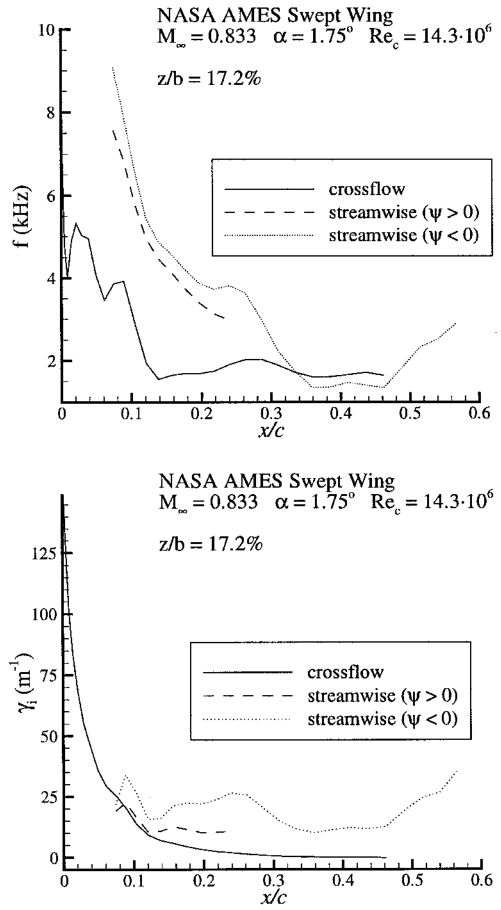

Fig. 6 Optimum frequency and spatial growth rate at z/b = 17.2%.

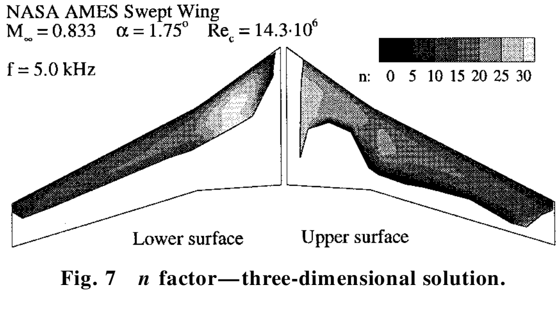

Fig. 7 n factor—three-dimensional solution.

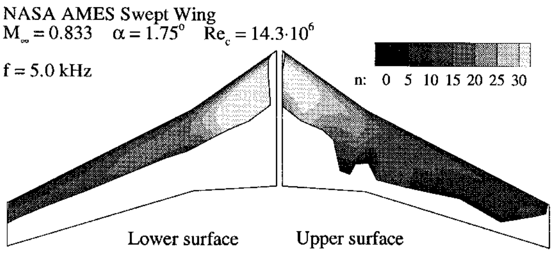

Fig. 8 ***n*** **factor—locally conical solution.**

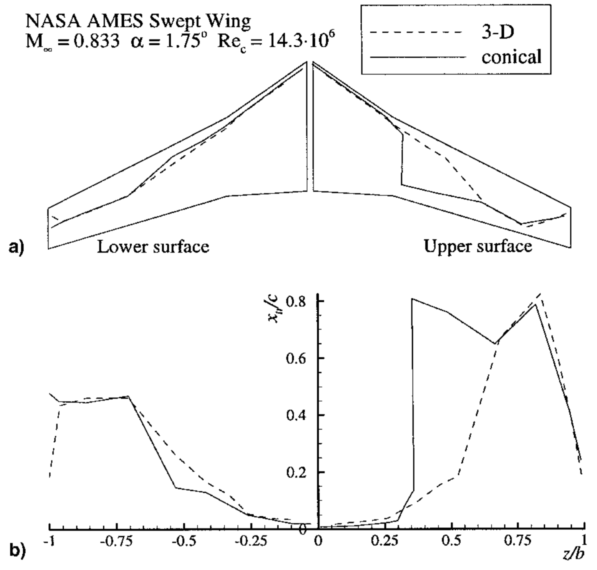

Fig. 9 Location of transition (n = 15, f = 5.0 kHz).

line based on this value, for both the fully three-dimensional and the locally conical solutions. On the outboard section of the suction side, the locally conical calculations do not reach the value $n = 15$, which explains the sudden aft-movement of the transition line there, corresponding to transition occurring at the shock. The n factor from the three-dimensional calculations also remains below 15 on part of the outboard section, but it still indicates a continuous transition line from wing root to wing tip, which corresponds more to what would be expected. The aft movement of the transition line is an effect of the decreasing local Reynolds number and takes place regardless of the particular value of n_{cr} chosen. Figure 9b shows that the differences between the two solutions are most significant on the upper surface of the wing, where the spanwise pressure gradients are most important. Even though these gradients are larger on the inboard section, it is on the outboard section that transition predictions most differ. Using a locally conical approach results in the two sections of the wing being treated as though they were two distinct wings, whereas the fully three-dimensional approach allows the influence of the inboard flow to be felt on the outboard flow stability characteristics.

ONERA-M6 Wing

The ONERA-M6 wing is a simpler geometry, with constant profile and sweep angles, no twist, and a low aspect ratio. The test case studied was $M_\infty = 0.84$, $\alpha = 3.06$ deg, and $Re_c = 11.7 \times 10^6$ (based on the mean chord, $c = 0.646$ m).[15] Figure 10 presents the complete picture of the n-factor growth at 25.0 kHz, which was found to be the critical frequency for this wing. This frequency is much higher than that found for the NASA AMES wing. The presence of a strong shock close to the leading edge meant that the laminar boundary-layer calculations could not proceed very far downstream. The n factors predicted by the locally conical solution are slighty higher than those resulting from the three-dimensional approach. Using the

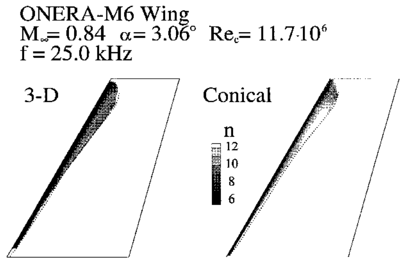

Fig. 10 ***n*****-factor evolution on ONERA-M6 wing.**

value of the critical n factor mentioned earlier, both solutions would however indicate that transition does not occur before the shock.

Conclusions

A stability analyzer for transition prediction over arbitrary three-dimensional wings operating in the transonic regime has been applied to the supercritical NASA AMES swept wing and the ONERA-M6 wing. A comparison of the present transition predictions with those obtained using conical-flow solutions has illustrated the importance of taking into account the spanwise pressure gradients, and thus of using fully three-dimensional flow solvers. The difference between the conical and fully three-dimensional results is of the same order of magnitude as that resulting from the inclusion of curvature or nonparallel effects, and it originates mainly from the different means of calculating the surface velocities. Calculations on wings with NLF profiles should further confirm these conclusions.

Acknowledgments

This work is supported by an R&D Grant of the Natural Sciences and Engineering Research Council of Canada, in collaboration with Bombardier Inc., Aerospace Group, and by the Fonds FCAR (Québec Government), through a Graduate Scholarship for M. Langlois. The authors would also like to express their gratitude to Fatih Tezok, Bombardier Aerospace Group, for the helpful discussions they had with him through the course of this project.

References

[1]Saric, W. S., "Physical Description of Boundary-Layer Transition: Experimental Evidence," *Special Course on Progress in Transition Modelling*, AGARD R-793, April 1993.

[2]Mack, L. M., "On the Stability of the Boundary Layer on a Transonic Swept Wing," AIAA Paper 79-0264, Jan. 1979.

[3]Malik, M. R., and Orszag, S. A., "Efficient Computation of the Stability of Three-Dimensional Compressible Boundary Layers," AIAA Paper 81-1277, June 1981.

[4]Arnal, D., "Établissement et résolution des équations de stabilité en écoulement compressible. Exemples de résultats," ONERA/Centre d'Études et de Recherches de Toulouse, TR 35/5018, Toulouse, France, Nov. 1986.

[5]Cebeci, T., and Stewartson, K., "Stability and Transition in Three-Dimensional Flows," *AIAA Journal*, Vol. 18, No. 4, 1980, pp. 398–405.

[6]Spall, R. E., and Wie, Y.-S., "Stability Theory and Transition Prediction Applied to a General Aviation Fuselage," *Journal of Aircraft*, Vol. 30, No. 2, 1993, pp. 161–167.

[7]Iyer, V., Spall, R. E., and Dagenhart, J. R., "Computational Study of Transition Front on a Swept Wing Leading-Edge Model," *Journal of Aircraft*, Vol. 31, No. 1, 1994, pp. 72–78.

[8]Masson, C., Martinuzzi, R., Langlois, M., Paraschivoiu, I., and Tezok, F., "Transition Prediction Capabilities for Conical Wings in the Transonic Regime," *Canadian Aeronautics and Space Journal*, Vol. 41, No. 1, 1995, pp. 28–39.

[9]Masson, C., Martinuzzi, R., Mirshams, M., and Paraschivoiu, I., "Natural Transition in Transonic Flows Using an Efficient Temporal/Spatial Formulation," *Journal of Aircraft*, Vol. 33, No. 5, 1996, pp. 931–937.

[10]Jameson, A., Schmidt, W., and Turkel, E., "Numerical Solutions of the Euler Equations by Finite Volume Methods Using Runge-Kutta Time-Stepping Schemes," AIAA Paper 81-1259, June 1981.

[11]Houdeville, R., Mazin, C., and Corjon, A., "Méthode de caractéristiques pour le calcul des couches limites tridimensionnelles," *La Recherche Aérospatiale*, No. 1993-1, 1993, pp. 37–49.

[12]Kaups, K., and Cebeci, T., "Compressible Laminar Boundary Layers with Suction on Swept and Tapered Wings," *Journal of Aircraft*, Vol. 14, No. 7, 1977, pp. 661–667.

[13]Mack, L. M., "Transition Prediction and Linear Stability Theory," *Laminar-Turbulent Transition*, CP-224, AGARD, May 1977.

[14]Arnal, D., "Boundary Layer Transition: Predictions Based on Linear Theory," *Special Course on Progress in Transition Modelling*, AGARD R-793, April 1993.

[15]*Test Cases for Inviscid Flow Field Methods*, AGARD AR-211, May 1985.

[16]Langlois, M., Masson, C., Paraschivoiu, I., and Tezok, F., "Curvature Effects in 3-D Compressible Transition Analysis," *Proceedings of the 3rd Annual Conference of the CFD Society of Canada (CFD95)* (Banff, Canada), 1995, pp. 315–322.

[17]Langlois, M., Casalis, G., and Arnal, D., "On the Practical Application of the PSE Approach to Linear Stability Analysis," *Aerospace Science and Technology* (to be published).